C. David Remy
ASL,
ETH Zürich

Keith Buffinton
Department of Mechanical Engineering,
Bucknell University

Roland Siegwart
ASL,
ETH Zürich

Stability Analysis of Passive Dynamic Walking of Quadrupeds

Abstract

We introduce a detailed numerical simulation and analysis framework to extend the principles of passive dynamic walking to quadrupedal locomotion. Non-linear limit cycle methods are used to identify possible gaits and to analyze the stability and efficiency of quadrupedal passive dynamic walking. In doing so, special attention is paid to issues that are inherent to quadrupedal locomotion, such as the occurrence of simultaneous contact collisions and the implications of the phase difference between front and back leg pairs. Limit cycles identified within this framework correspond to periodic gaits and can be placed into two categories: in-phase gaits in which front and back legs hit the ground at roughly the same time, and out-of-phase gaits with a $\pm 90^\circ$ phase shift between the back and front leg pairs. The latter are, in comparison, energetically more efficient but exhibit one unstable eigenvalue that leads to a phase divergence and results in a gait-transition to a less efficient in-phase gait. A detailed analysis examines the influence of various parameters on stability and locomotion speed, with the ultimate goal of determining a stable solution for the energy-efficient, out-of-phase gait. This was achieved through the use of a wobbling mass, i.e. an additional mass that is elastically attached to the main body of the quadruped. The methods, results, and gaits presented in this paper additionally provide a point of departure for the exploration of the considerably richer range of quadrupedal locomotion found in nature.

The International Journal of Robotics Research
Vol. 00, No. 00, Xxxxxxxx 2009, pp. 000–000
DOI: 10.1177/0278364909344635

Figures 1, 3–7, 9, 10 appear in color online: http://ijr.sagepub.com

KEY WORDS—dynamics; mechanics, design and control of legged robots; mechanics, design and control of underactuated robots.

1. Introduction

A new paradigm in the control of walking machines considers stability and gait creation less as a continuous-time problem but rather by looking at the entire gait cycle as a single entity. This is a particularly fruitful approach to the study of *passive dynamic locomotion* in which most of a system's degrees of freedom are allowed to move freely and simply follow their natural dynamic motions, while the periodicity (and therefore stability) of the gait is only monitored at distinct instances. This idea of exploiting natural dynamics rather than imposing specific kinematic trajectories leads to an extremely efficient gait as it does not require actuators to perform negative work associated with tracking a nominal trajectory. This becomes especially important in the presence of disturbances: instead of actively resisting them to stay on a nominal trajectory, deviations from the periodic motion are tolerated and the natural dynamics are used to damp out the disturbances over the course of several steps of motion.

These principles emerge most impressively in so-called *passive dynamic walkers*. These walkers are simple mechanical mechanisms that do not possess actuation or sensing of any kind but in essence use the dynamics of coupled pendula to walk down a shallow incline. The most striking property of these mechanisms is the fact that for a well-selected set of parameters (link masses and inertial properties) the motion is dynamically stable. Even in the presence of small disturbances, the mechanism is able to walk continuously while maintaining a steady step length and forward speed. McGeer (1990a) was the first to describe these concepts in his seminal paper

on passive dynamic walking. Since then, these principles have been extended to mechanisms with knees (McGeer 1990b) and to walkers that move stably in three dimensions (Collins et al. 2001). Passive dynamic stability has also been shown to assist human walking (Bauby and Kuo 2000). Members of the robotic community have incorporated these principles into a succession of prototype walkers (Collins et al. 2005; Dertien 2006; Wisse et al. 2007) and demonstrated how to add actuation without drastically impeding the natural dynamics. This is important to achieving powered walking on level ground and allows for directional control of these very efficient walkers.

The application of these principles to quadrupedal locomotion, however, has drawn far less attention. Smith and Berkemeier (1997) are, to the best of the authors' knowledge, the only researchers who have analyzed the implications of passive dynamics to true quadrupedal walking. Their principal finding was the identification of two stable passive dynamic walking gaits: a two-beat gait in which the front and back feet move in phase, and a four-beat gait in which they move 90° out of phase. The latter is energetically more efficient, as less energy is lost in collisions, but appeared to be unstable for a reasonable range of parameter variations.

Based on their work, a detailed simulation framework was created to comprehensively study passive dynamic gaits of quadrupeds. We assessed the stability of various gaits and quantified the potential energy savings of the four-beat quadruped gait. The "efficiency" of a particular gait is expressed through the maximal achievable walking speed on a given slope. This measure of efficiency was chosen rather than the nominal *cost of transportation* (CoT) since the CoT depends solely on the inclination of the slope and hence is not suited for direct comparisons of passive dynamic walkers. The primary focus of our work is to investigate means of stabilizing the energetically more efficient four-beat quadruped gait. This was ultimately achieved through the use of a *wobbling mass* that was added to the main body of the quadruped.

2. Multi-body Quadrupedal Model

For the purposes of this study, a quadruped was modeled as a planar multi-body system (Figure 1). The main body and the legs are represented by five rigid links with distributed mass that are connected by rotational joints at the hip and shoulder. Feet were modeled as points with no geometrical extension (sacrificing performance for simplicity in comparison to curved feet (Adamczyk et al. 2006)). During contact, the feet are consequently modeled as simple rotational joints that connect the stance legs to a fixed point on the ground. The swing legs move freely around the hip and shoulder, respectively, giving the system a total of three degrees of freedom. Joint friction was not modeled and thus energy losses only occur during ground collisions. To compensate for these losses and to maintain a steady walking speed, walking on a shallow slope was

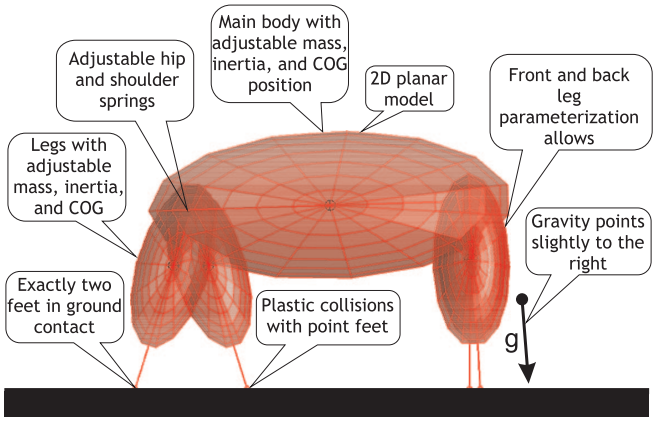

Fig. 1. Model of a passive dynamic quadruped. The two stance feet are effectively pinned to the ground, which gives the model the dynamics of a four-bar linkage with two additional links (the swing legs) attached to hip and shoulder joints.

simulated by pointing the gravity vector slightly to the right of vertically downwards. An extension used here to the mechanics of the passive dynamic bipeds described by McGeer is the inclusion of hip and shoulder springs. These are torsional springs that connect the stance and swing legs of each leg pair. They are not connected to the main body and produce equal and opposite torques on the legs.

All units in the system model were normalized (Hof 1996) with respect to leg length l and total mass M. The gravitational constant was set equal to one, which has the advantage that velocities are expressed in the units of $\sqrt{gl}$ which means that their value is equal to the square root of the Froude number (Vaughan and O'Malley 2005). The remaining parameters of our model roughly correspond to the dimensions and mass properties of a Merino sheep (Table 1). The equations of motion for this system were derived and numerically integrated using MATLAB/Simulink and the SimMechanics toolbox (The MathWorks, Natick, MA). This toolbox uses a relative coordinate formulation together with recursive computational procedures to compute the equations of motions (Wood and Kennedy 2003). Numerical integration was performed with a Runge–Kutta method using the Dorman–Price (4, 5) pair (Shampine and Reichelt 1997). During integration total system energy was monitored to detect numerical errors.

3. Collision Modeling

The contact events at foot strike were modeled as fully inelastic collisions such that the point of contact of the impacting foot comes to a complete stop after the collision while the corresponding stance foot leaves the ground at the same time. If the swing foot reaches the ground plane while moving in the

Table 1. Parameter values of the quadruped model are given in units normalized relative to total mass and leg length. The proportions of the model roughly represent the dimensions and mass properties of a Merino sheep. Ground inclination was selected to create a walking speed similar to that used by Merino sheep.

Total mass	$1M$
Leg length	$1l$
Main body mass	$0.8M$
Main body length	$1.5l$
Main body radius of gyration	$\sqrt{1/10}$ main body length
Main body COM position	Center
Leg mass	$0.05M$
Leg radius of gyration	$\frac{2}{3}\sqrt{1/10}l$
Leg COM position	$\frac{1}{3}l$ below joints
Ground inclination	1°
Hip/shoulder spring stiffness	$0\ Mgl/\text{rad}$

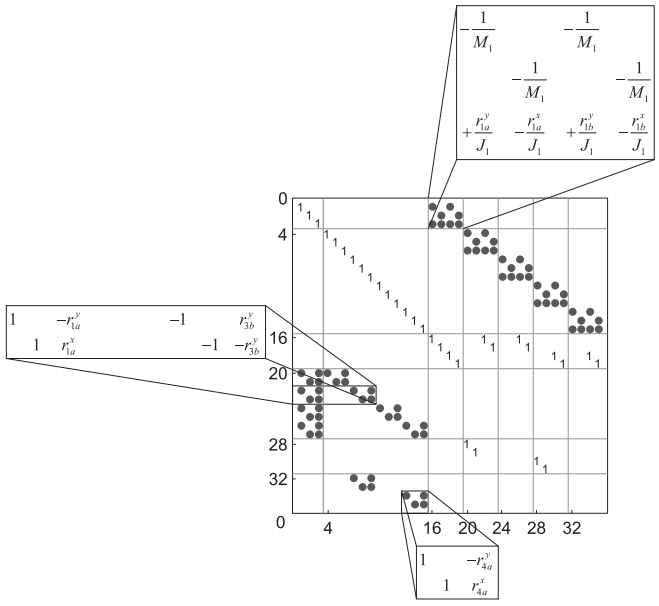

Fig. 2. Structure of the coefficient matrix **A** that is used to compute the changes in velocities during collisions. In this specific example, the contacts at legs 2 and 3 are open/opening, while the contacts of legs 4 and 5 are closed/closing.

negative y-direction, the integration of the equations of motion is stopped and the computation of post-impact velocities is triggered. As we are dealing with a knee-less model, collision detection is limited to states in which the swing foot is in front of the corresponding stance foot. This prevents (numerical) foot scuffing during swing and the untimely termination of the simulation.

Collision dynamics were developed from the impulse–momentum relations describing the velocity changes of the individual segments, expressed in Cartesian coordinates, along with the constraints describing the impulse balances and kinematic coupling in the joints and points of contact to produce a total of 35 linear equations in 35 unknowns (15 velocities and 20 impulses). They are stated in matrix form as $\mathbf{Ax} = \mathbf{b}$, where $\mathbf{x} = (\dot{x}_1^+ \ \ \dot{y}_1^+ \ \ \omega_1^+ \ \ \ldots \ \ \omega_5^+ \ \ I_{1a}^x \ \ I_{1a}^y \ \ \ldots \ \ I_{5b}^y)^{\mathrm{T}}$ is a vector composed of the unknown velocities after impact and the impulsive forces, and $\mathbf{b} = (\dot{x}_1^- \ \ \dot{y}_1^- \ \ \omega_1^- \ \ \ldots \ \ \omega_5^- \ \ 0 \ \ \ldots \ \ 0)^{\mathrm{T}}$ is a vector containing the known pre-impact velocities padded with zeros. The coefficient matrix **A** is sparse (Figure 2). The post-impact velocities $\mathbf{v}^+$ are calculated from a vector of pre-impact velocities $\mathbf{v}^-$ using the equation:

$$\mathbf{v}^+ = \overline{\mathbf{A}^{-1}}\mathbf{v}^- \tag{1}$$

with $\overline{\mathbf{A}^{-1}}$ containing solely the upper left 15×15 elements of $\mathbf{A}^{-1}$. After each exchange of stance and swing legs, the next step of the numerical integration of the equations of motion is begun again with the newly computed velocities.

3.1. Simultaneous Collisions

An important consideration in quadrupedal walking is a clear understanding and analysis of the effect of the sequence, or simultaneity, of the collision impacts corresponding to each of the footfalls. When the time between two contact events becomes infinitesimally small, the geometrical properties of the system and the velocities of the links remain unchanged between the first collision and the second. All changes in velocities can therefore be understood by considering the sequence of matrix operations presented in (1). The primary collision is described either by a matrix $\mathbf{A}_{\text{Front}}$ or $\mathbf{A}_{\text{Back}}$, depending on which swing foot hits the ground first. The second collision matrix ($\mathbf{A}_{\text{Both}}$) is identical in both cases, as an exchange of stance and swing foot has occurred both in the front and back leg pairs. It is, in fact, possible to use solely this matrix to simulate a truly simultaneous collision, in which both pairs of legs (front and back) exchange support at the same moment (which is a rather theoretical situation). Depending on the order (or simultaneity) of the contact events, the post-collision velocities must be expressed in one of the following three ways:

$$\mathbf{v}^+ = \overline{\mathbf{A}_{\text{Both}}^{-1}\mathbf{A}_{\text{Front}}^{-1}}\mathbf{v}^-, \quad \text{for the order } \textit{front leg}, \textit{back leg}, \tag{2}$$

$$\mathbf{v}^+ = \overline{\mathbf{A}_{\text{Both}}^{-1}}\mathbf{v}^-, \quad \text{for a truly simultaneous collision}, \tag{3}$$

$$\mathbf{v}^+ = \overline{\mathbf{A}_{\text{Both}}^{-1}\mathbf{A}_{\text{Back}}^{-1}}\mathbf{v}^-, \quad \text{for the order } \textit{back leg}, \textit{front leg}. \tag{4}$$

The computation of the post-impact velocities consequently depends strongly on the (numerical) determination of order of contact or simultaneous contact. The implications of this are described in more detail in Section 5.1.

4. Limit Cycle Analysis

Throughout our study, the following seven state variables constitute the state vector $\mathbf{x}$.

- Angles of the back stance leg and the two swing legs. All angles are expressed with respect to the vertical.
- Angular velocities of these three legs.
- Distance between front stance foot and back stance foot points of contact (this state variable has a derivative of zero and is only altered at the transfer of support).

With these coordinates, the search for a periodic gait can be seen as the identification of a limit cycle in the seven-dimensional state space of the robot. A Poincaré section based on the back foot ground contact was used to define a stride-to-stride transfer function $\mathrm{P}(\cdot)$, mapping a vector of initial states $\mathbf{x}^k$ at the beginning of a half stride to the states at the beginning of the next half stride according to $\mathbf{x}^{k+1} = \mathrm{P}\left(\mathbf{x}^k\right)$. A numerical root search was used to identify initial conditions $\mathbf{x}^*$ that resulted in a periodic gait (i.e. when $\mathrm{P}\left(\mathbf{x}^*\right) - \mathbf{x}^* = 0$).

For a small disturbance $\Delta\mathbf{x}$ to a periodic initial condition $\mathbf{x}^*$, the stride-to-stride transfer function can be linearly approximated by $\mathrm{P}\left(\mathbf{x}^* + \Delta\mathbf{x}\right) \approx \mathbf{x}^* + \mathbf{J}\Delta\mathbf{x}$, where $\mathbf{J}$ is the Jacobian (the monodromy matrix) of the transfer function. A disturbance close to a periodic solution evolves according to the relation: $\Delta\mathbf{x}^{k+1} \approx \mathbf{J}\Delta\mathbf{x}^k$. If the magnitude of all eigenvalues (the Floquet multipliers) of $\mathbf{J}$ is smaller than one, any disturbance will vanish over time and the limit cycle is considered stable. If at least one eigenvalue has a magnitude larger than one, the system is unstable. As a disturbance parallel to the solution vector of the actual limit cycle will be completely eliminated within a single stride, one of the eigenvalues will always be zero. For this reason only the six non-zero eigenvalues are reported throughout this paper.

5. Periodic Gaits

The limit cycles (or periodic gaits) that were identified can be placed into two categories: gaits in which front and back legs hit the ground at the same time (or roughly the same time) and gaits with a $\pm 90^\circ$ phase shift between the back and front leg pair. For other phase shifts no periodic solutions were obtained. In the simplified planar and symmetric model used here, no difference between left and right legs, or a positive and a negative phase shift, exists. The range of possibilities for footfall sequences (Figure 3) can thus be reduced to the notion of either an in-phase "two-beat" gait or a 90° out-of-phase "four-beat" gait. We preferred the terms two-beat gait and four-beat gait to more established zoological terms (such as "trot", "pace", "amble", or "single-foot gait"), as these terms tend to suggest certain properties and characteristics that are not represented in our simplified model.

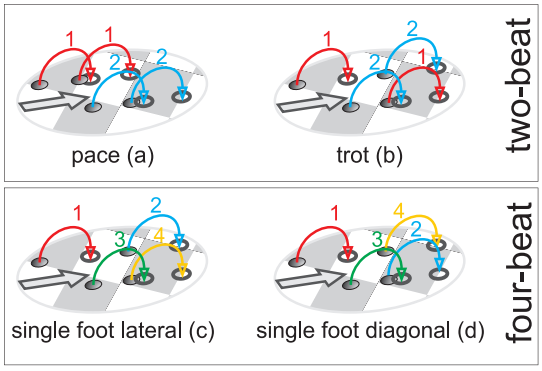

Fig. 3. Periodic gaits found for the passive dynamic quadruped can be classified into gaits in which two feet strike the ground at roughly the same time (the *pace* shown in (a) and the *trot* in (b)) and gaits in which the feet strike the ground in an evenly spaced sequence (the *lateral single foot gait* in (c) and the *diagonal single foot gait* in (d)). For gaits corresponding to other motion phase shifts, no periodic solutions are obtained. Note that in the simplified planar model used here, no difference between a trot and a pace and between a lateral and a diagonal sequence exists. Gaits (a) and (b) are thus referred to as "two-beat" and gaits (c) and (d) as "four-beat".

5.1. Two-beat Gait

A truly exact two-beat gait is a mere theoretical construct: if front and back legs of the quadruped model are exactly in phase, identical forces and impulses act on both ends of the connecting link (main body). No work is transmitted from one leg pair to the other through the main body and the quadruped behaves like two independent bipeds, each carrying half the mass of the quadruped's main body. For the parameters of our model, this results in a normalized walking speed of 0.184 $\sqrt{l \cdot \mathrm{g}}$ on a 1° slope.

A single passive dynamic *biped* modeled in this way walks stably, and a Floquet analysis shows that its eigenvalues have a magnitude smaller than one (Table 2 and Figure 4). If two identical bipeds are connected to form a quadruped with an exact two-beat gait, however, the slightest disturbance eliminates the (only theoretically possible) exact simultaneity of their contact collisions. In this case, the collisions must now be processed in

Table 2. Eigenvalues and forward velocities of an inexact two-beat gait of a quadruped, a four-beat gait of a quadruped, and a stable gait of a biped with corresponding system parameters.

Gait	Quadruped		Biped
	Two-beat	Four-beat	
Eigenvalues	$0.060 + 0.851i$	$-0.030 + 0.005i$	$-0.416 + 0.422i$
	$0.060 - 0.851i$	$-0.030 - 0.005i$	$-0.416 - 0.422i$
	$0.460 + 0.395i$	$0.128 + 0.602i$	0.046
	$0.460 - 0.395i$	$0.128 - 0.602i$	–
	0.012	0.086	–
	0.025	**2.381**	–
Velocity	$0.202\sqrt{l \cdot g}$	$0.224\sqrt{l \cdot g}$	$0.184\sqrt{l \cdot g}$

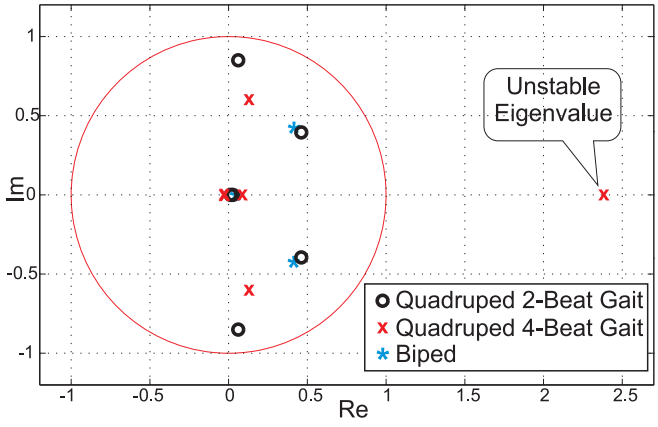

Fig. 4. Overlaid root locus plots of the eigenvalues of the monodromy matrix of an inexact two-beat gait of a quadruped, a four-beat gait of a quadruped, and the stable gait of a biped with corresponding system parameters. The small differences in root locus locations of bipedal and two-beat gaits are due to the coupling of contacts in the quadruped that result in a small phase shift between back and front leg pairs. Note that the four-beat gait has one unstable eigenvalue.

sequence, and the computation will result in completely different post-impact velocities (Table 3). This means that the stride-to-stride transfer function of the exact two-beat gait is discontinuous with respect to changes in the initial states. No derivative of the transfer function exists, and the Jacobian cannot be computed, making it impossible to apply Floquet analysis to this gait and quantitatively assess its stability. Nevertheless, since the exact two-beat gait will depart from a stable limit cycle as a result of even the smallest disturbance, it can be considered unstable for all practical purposes. If an exact two-beat gait were required in an actual physical system, the only way to achieve it would be through the introduction of a mechanical linkage that keeps the two leg pairs exactly in phase (Osuka and Kirihara 2000).

Beyond the exact two-beat gait, there exist two inexact two-beat solutions in which the feet strike the ground not exactly simultaneously, but rather in quick succession. The results presented here were achieved with the footfall order "front foot–back foot". The eigenvalues and walking velocity for the other gait (with an opposite order of contact) are nearly identical and not reported separately. Even though there are in fact four independent foot strikes, we refer to this gait as a two-beat gait, as the time between the two successive strikes accounts for less then 0.2% of the total stride time. This gait is slightly faster than the exact two-beat gait ($0.202\ \sqrt{l \cdot g}$ as compared with $0.184\ \sqrt{l \cdot g}$) as less energy is lost in ground contact collisions. All eigenvalues of the monodromy matrix have a magnitude smaller than one (Table 2 and Figure 4) and thus the inexact two-beat gait is stable.

To better understand the greater velocity and the lower energy loss of the inexact two-beat gait, consider that with simultaneous collisions the velocity of the center of mass (COM) of a point mass system can be shown to be redirected at impact with a collision angle of 2α (where α is identical to the stance leg angle). For this conceptual model, the post-impact velocity of the COM is $v^+ = \cos(2\alpha)\, v^-$ (cf. McGeer (1990a) with $r_{gyr} = 0$), yielding an energy loss of 17.7% for the given gait. If the collisions happen in quick succession, however, the COM is redirected twice with a collision angle of only α each time, leading to $v^+ = \cos^2(\alpha)\, v^-$ and corresponding to an energy loss of only 9.1%. For our non-point mass model, the actual energy losses (Table 3) are higher, due to the additional losses associated with the distributed mass of the system and the rotational motion of the main body between the two collisions.

5.2. Four-beat Gait

In a four-beat gait, the front (or back) foot strike occurs at the moment at which the hip (or shoulder) is at the highest point of its arc of motion. The main body COM thus undergoes a smaller vertical excursion over the course of a stride than the

Table 3. Post-impact velocities of an exact two-beat gait are compared for different orders of contact. The pre-impact angles and velocities are equal in all three cases. The different outcomes depend solely on the order in which the contact events are processed.

	Back contact first	Front contact first	Simultaneous contact
Back stance leg	$-0.269\text{rad}/\sqrt{l/g}$	$-0.269\text{rad}/\sqrt{l/g}$	$-0.261\text{rad}/\sqrt{l/g}$
Back swing leg	$-0.188\text{rad}/\sqrt{l/g}$	$-0.198\text{rad}/\sqrt{l/g}$	$-0.173\text{rad}/\sqrt{l/g}$
Front swing leg	$-0.198\text{rad}/\sqrt{l/g}$	$-0.188\text{rad}/\sqrt{l/g}$	$-0.173\text{rad}/\sqrt{l/g}$
Energy dissipation (percentage of total)	14.8%	14.8%	19.5%

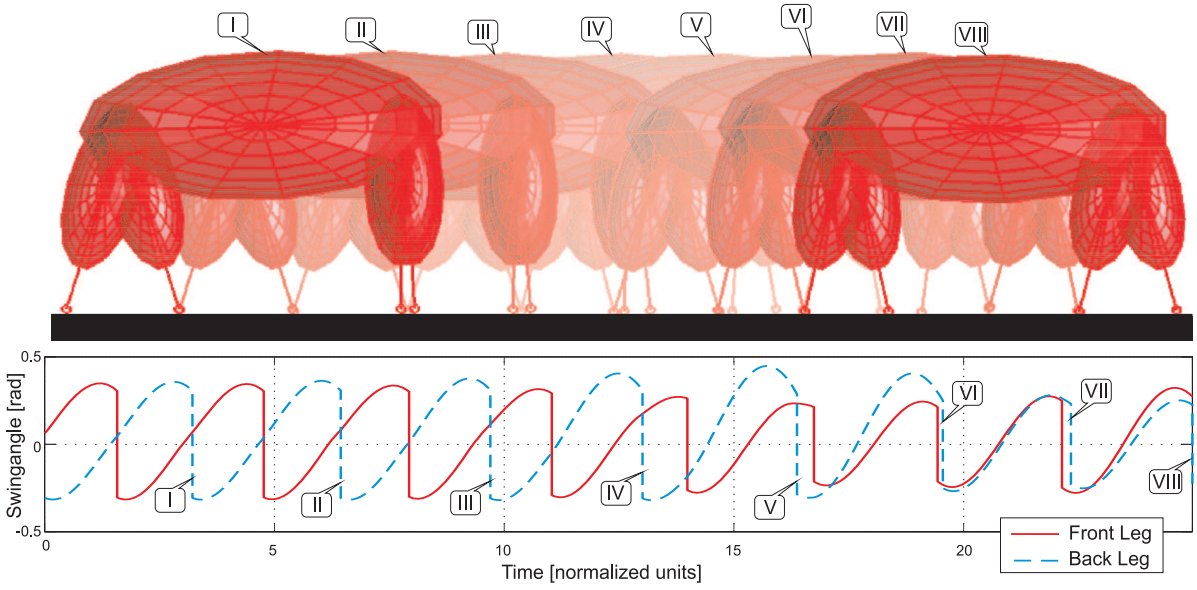

Fig. 5. Passive transition from a slightly disturbed four-beat gait into an inexact two-beat gait. The bottom graph shows how the angles of the front swing leg and back swing leg evolve over time. It can be clearly seen that the motion of the two legs become synchronized over just a few of steps. The discontinuities in the graph indicate the transfer of support at foot strike, when the roles of stance and swing legs are exchanged. The upper portion of the figure shows overlaid video frames for the eight successive back foot strikes.

two-beat gait, which results in smaller fluctuations in the forward velocity. As the velocities are always highest right before impact, the four-beat gait can achieve a higher average speed over the course of a stride while maintaining the same impact velocities (and therefore impact losses) as the two-beat gait. In other words, in the four-beat gait a higher fraction of the system energy is stored as potential energy at the moment of impact. This means that the total energy in the system (and therefore the walking speed) is increased while maintaining the same amount of kinetic energy (which determines the losses at impact). For our system, the four-beat gait achieves a higher walking speed of $0.224\sqrt{l \cdot g}$ as compared with a speed of $0.202\sqrt{l \cdot g}$ for the two-beat gait on the same slope.

Unfortunately, while the two-beat gait is dynamically stable, the four-beat gait has one unstable eigenvalue. This eigenvalue corresponds to the "phase mode" described by Smith and Berkemeier (1997) and affects the phase shift between back and front legs (Table 2 and Figure 4). Consequently, a small disturbance to the four-beat gait will cause the system to deviate from its $\pm 90^\circ$ phase difference and transition from the four-beat gait to the two-beat gait (Figure 5). Efforts to stabilize the four-beat gait and thus to realize its inherent efficiency are described in Section 6.

6. Stabilization of the Four-beat Gait

6.1. Parameter Variation

To examine the influence of the model parameters on walking speed and the eigenvalues of the monodromy matrix, a number of parameter variations were studied. Using the base parameter

set given in Table 1, parameter ranges were selected such that a periodic four-beat gait could be identified for all parameter variations. The following parameters were examined.

(a) *Leg mass.* The relationship between leg and body mass was varied such that a single leg contributed between 0.5% and 20% of the total mass. Moment of inertia values of legs and main body were adjusted accordingly. Making the legs lighter (in relation to the over all mass) increased the walking speed and decreased the magnitude of the unstable four-beat phase-mode eigenvalue (Figure 6-I).

(b) *Main body length.* The length of the main body was varied between $0.2l$ and $10l$. The main body inertia was adjusted accordingly. Walking speed and eigenvalue positions remained almost constant. Less than 1% variation in walking speed was observed throughout the entire parameter range.

(c) *Main body COM position.* The COM of the main body was shifted along its anteroposterior axis. It was displaced by $\pm 0.5l$ with respect to a centered position. Introducing this asymmetry increased the unstable phase-mode eigenvalue and reduced the walking speed of the four-beat gait (Figure 7-I).

(d) *Leg COM position.* The COM of all legs was displaced along the leg in the range of $\pm 0.25l$ from its nominal position at $\frac{1}{3}l$ below the joints. Walking speed peaked at $0.231\ \sqrt{l \cdot \mathrm{g}}$ for a COM position of $0.210l$ below the joints.

(e) *Ground inclination.* The inclination of the ground slope was altered in the range of 0.01° to 10°. Steeper slopes resulted in a higher walking speed and a less unstable phase mode with a corresponding eigenvalue closer to 1. Note, however, that the other modes became unstable for inclinations over 2.3° (Figure 6-III).

(f) *Asymmetry with respect to the leg mass*. The mass of the front legs was changed in the range of $0.02M$ to $0.08M$. The mass of the back legs was correspondingly changed an equal amount in the opposite direction, such that the overall mass M of the system remained constant. Moments of inertia of the legs were adjusted accordingly. Introducing this asymmetry slightly increased the magnitude of the phase mode eigenvalue (by 6%). The other eigenvalues and the walking speed remained virtually constant. Speed reduction with respect to the symmetric configuration was less than 1%.

(g) *Asymmetry with respect to the leg length*. The front legs were extended (or shortened) in the range of $\pm 0.15l$ while the back legs were correspondingly shortened (or extended). The average leg length remained l. Inertia values of the legs were adjusted accordingly. Again, the most symmetric configuration resulted in the smallest and least unstable phase-mode eigenvalue. In contrast to other front–back asymmetries, however, walking speed did not peak for the symmetric configuration. This can be attributed to the inclined attitude of the main body that results from the different leg lengths. Depending on the main body's inclination, the impacts at foot strike act either dominantly translational (if the front legs are shorter) or rotational (if the front legs are longer) on the main body. The latter results in lower energy losses, as the rotational inertia of the main body is effectively smaller than the translational inertia (i.e. the radius of gyration is smaller than the moment arms of the translational inertias). Walking speed increases as the front leg length increases (Figure 7-II).

(h) *Asymmetry with respect to the leg COM position.* The position of the front leg COM was displaced along the leg in the range of $\pm 0.25l$ from its nominal position while the COM of the back leg was correspondingly moved the same amount in the opposite direction. The asymmetry increased the magnitude of all eigenvalues and reduced the speed of the walker (by 9%). The root locus plot and velocity graph are conceptually similar to those obtained by changing the position of the COM of the main body.

(i) *Hip and shoulder spring stiffness*. The stiffness of the torsional hip and shoulder springs was varied from 0 to 1.0 Mgl/rad. With increasing stiffness, these springs were able to decrease the instability of the phase-mode eigenvalue while increasing the model's walking speed (Figure 6-IV). Increasing the hip stiffness leads to shorter steps, which in turn reduces the impact losses and allows for ever-increasing walking velocity.

For none of these variations was a stable four-beat gait identified. This is consistent with Smith and Berkemeier's claim that "... this ['phase'] mode is almost invariably unstable...". Nevertheless, two general trends could be observed throughout the study.

(1) Parameter variations that yielded higher speeds corresponded to a smaller and thus less unstable phase-mode eigenvalue. This was seen in all symmetric cases, as discussed below, and additionally included making the legs lighter (case a), the main body shorter (case b), increasing the inclination angle of the slope (case e), and increasing the stiffness of the hip and shoulder springs (Figure 6).

(2) Asymmetry of the model always increased the values of the unstable phase-mode eigenvalue and in most cases reduced walking speed. Differences between the front

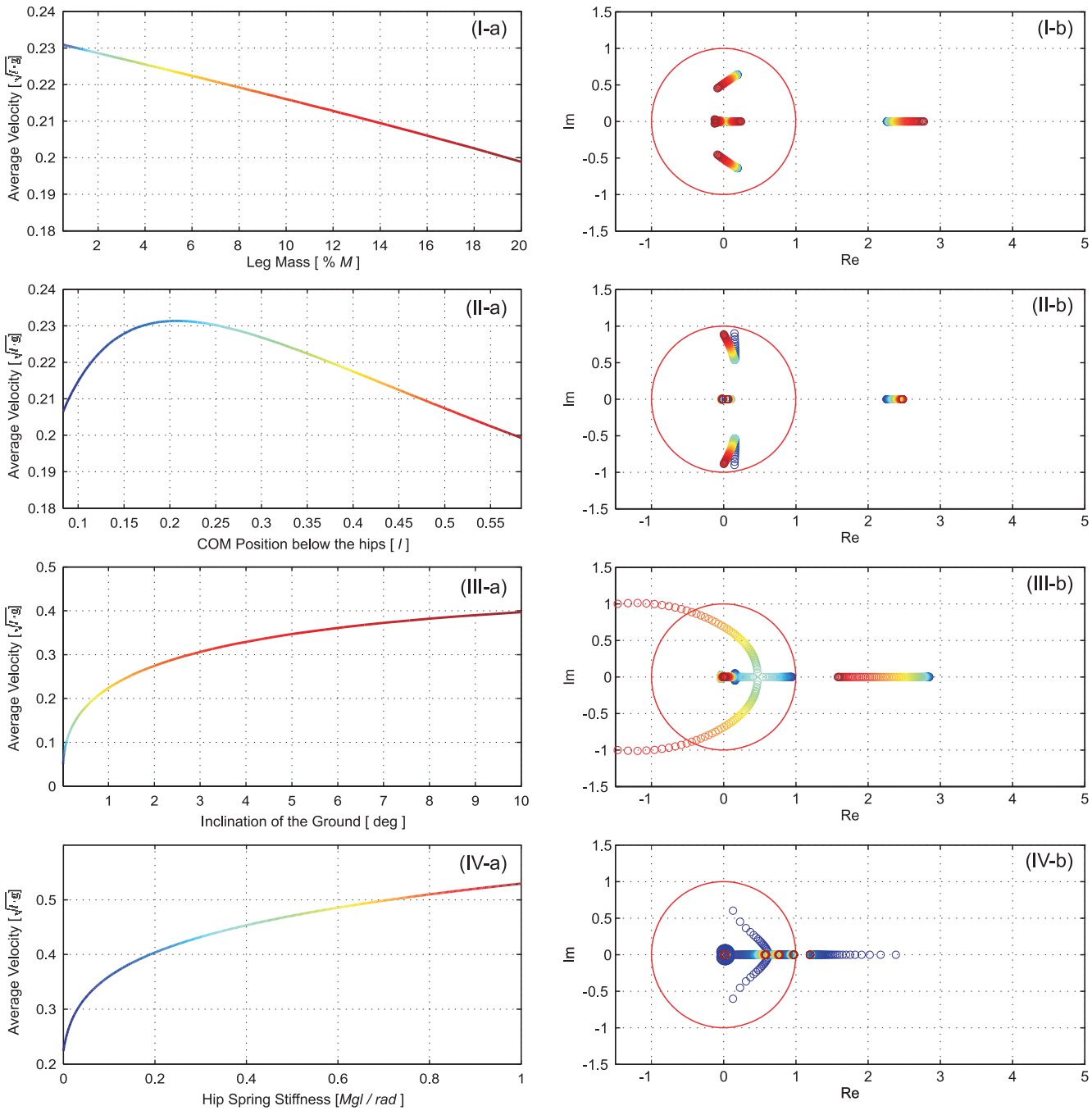

Fig 6. (a) The walking speed and (b) the positions of the six eigenvalues when varying the mass of the legs (I), for varying locations of the COM of the legs (II), for increasing the steepness of the incline on which the system walks (III), and for increasing stiffness of the torsional hip and shoulder springs (IV). Note that data markers of the same color in the (a) and (b) plots correspond to the same set of system parameters. As a general trend, parameter variations that increase walking speed tend to decrease the phase-mode eigenvalue and make it less unstable. In these examples, this holds for lighter legs, for an optimal COM position of $0.210l$ below the joints (where walking speed peaked at $0.231\ \sqrt{l \cdot g}$), for a steeper inclination of the ground, and for stiffer hip and shoulder springs. All of these configurations diminished the instability of the phase mode but are not able to reduce its eigenvalue to less than one.

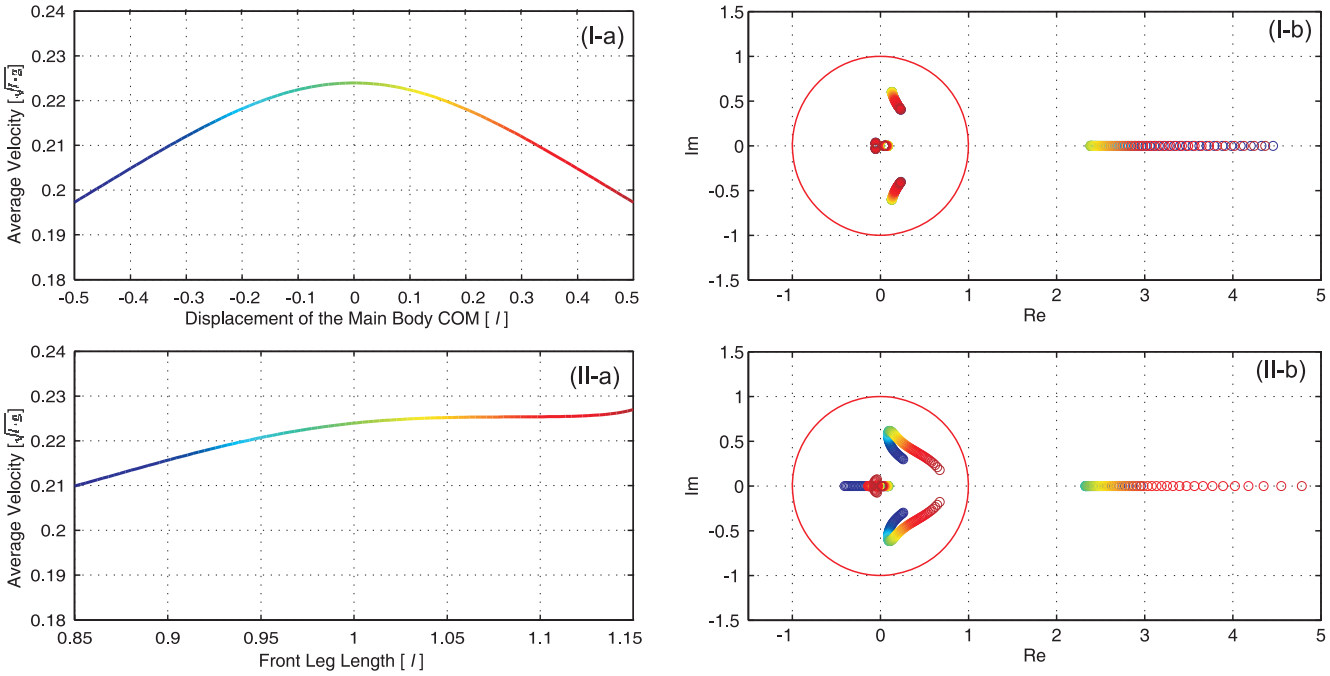

Fig 7. Asymmetries with respect to the anteroposterior axis generally increased the values of the unstable eigenvalues and in most cases reduced the walking speed. Shown as examples are the variation of the COM position of the main body (I) and the influence of different leg lengths (II). In both cases, the most symmetric configuration resulted in the smallest and least unstable phase-mode eigenvalue, as can be seen in the root locus plots in (I-b) and (II-b). In general, symmetry also resulted in the fasted walking speed, as can be seen in (I-a). Similar results were obtained when introducing asymmetry in the mass of the legs or the position of the leg COM. However, when considering leg length, walking speed does not peak in the symmetric configuration (II-a). This can be attributed to the inclined attitude of the main body, in which the impacts at foot strike act on the main body either predominantly translationally (for shorter front legs) or rotationally (for longer front legs). The latter is accompanied by lower energy losses and results in higher walking speeds. Data markers of the same color in the (a) and (b) plots correspond to the same set of system parameters.

and the back ends of the model inevitably moved the phase-mode eigenvalue further away from the unit circle and peak speed was mostly achieved with a symmetric configuration with the only exception of asymmetry in the leg length (Figure 7). This was observed when displacing the position of the main body COM (case c), as well as when changing the properties of the individual legs (as in cases f, g, and h). As described in more detail in Section 7, this was an unexpected result since significant differences between front and back leg pairs are present in almost all biological quadrupeds and may be a result of the limitations of our model.

With the goal of stabilizing the phase-mode eigenvalue, hip and shoulder springs were the most promising modification. This is consistent with studies on bipedal robots that have also reported a beneficial effect of hip springs on stability and walking speed. Kuo (1999) for example stated, “Speed increases roughly linearly with spring stiffness . . . The unstable eigenvalues also decrease in magnitude with increasing spring stiffness.”. In quadrupeds, increasing the stiffness of the hip and shoulder springs also increases the amount of energy that is stored within a leg pair (and is periodically exchanged between the two legs of that pair). This means that the relative importance of the dynamic coupling (between the ground impacts and the dynamics of the main body) is diminished and the synchronizing effect of these dynamics is reduced. The inability of all of the parameter studies described above to produce a stable four-beat gait led us to consider a more significant change to the structure of the system, as is described in detail below.

6.2. Wobbling Mass

Even though none of the cases of the previous section yields a phase-mode eigenvalue less than one, the results do suggest an optimal set of parameters that minimizes the magnitude of the phase-mode eigenvalue as much as possible, for example, by using a symmetric model with lightweight legs, a short main

body, an optimized COM position in the legs, and high stiffness hip and shoulder springs. For practical applications the remaining instability would then pose a relatively minor control challenge. Disturbances would grow slowly, leaving a controller ample time to eliminate them.

An active controller, however, is not desirable within the present context of developing a truly passive dynamic system. Even if very little controller intervention is required, any actuation will inevitably affect the natural dynamics of the system, introduce unwanted energy losses, and potentially negatively affect the dynamic stability of other modes. Instead of designing an active control scheme, an attempt was made here to augment the system with additional passive elements. To minimize any undesired influence on the other passive dynamic modes, we limited our efforts to modifications of the main body.

A successful solution was achieved through the inclusion of a *wobbling mass* (Figure 8). "Wobbling masses" (e.g. Liu and Nigg (2000)) are present in all biological vertebrates and correspond to muscles and other tissue not rigidly connected to bone that are thus able to move elastically within certain limits. To emulate such a wobbling mass, half the mass of the main body (equal to 40% of the total weight of the system) was separated from the main body link and elastically reattached via a spring–damper element. To keep the model as simple as possible, the wobbling mass was only allowed to translate relative to the main body along its anteroposterior axis; motion in all other directions was constrained. This modification adds an additional degree of freedom to the model, corresponding to the relative motion between the wobbling mass and the main body. Two additional states (the displacement of the wobbling mass and the rate of displacement) were added to the system's state space. The limit cycle analysis was then modified accordingly.

The wobbling mass stabilized the phase-mode eigenvalue of the four-beat gait for spring stiffnesses between 1.4 and 2.3 Mg/l with no damping (Figure 9-I). In contrast to the parameter studies described above, several distinct groups of solutions were found within the overall range of spring stiffnesses yielding stable four-beat responses. The groups can be easily identified within Figure 9-I by the discontinuities in the walking velocity, and the gaps between the groups can be attributed to resonance interactions of the wobbling mass with the periodic walking motion. The first discontinuity at a stiffness of around 1.4 Mg/l corresponds to a resonance case in which the natural frequency of the wobbling mass swinging relative to the remaining mass is matched with the strides of the quadruped. For the given parameters, the stride frequency of the passive dynamic walker ω_{stride} is 2.35 rad/$\sqrt{l/g}$. For a simplified model in which the wobbling mass m_{wob} and the entire remaining mass m_{rem} swing freely with respect to each other, the natural frequency ω_o of the wobbling mass oscillation can be expressed as

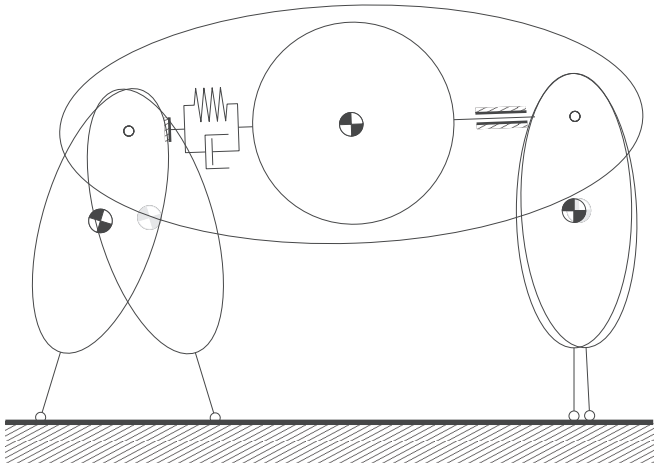

Fig. 8. To stabilize the passive dynamic four-beat gait, a wobbling mass was added to the model. Elastically attached to the main body segment, the mass moves along the anteroposterior axis of the main body.

$$\omega_o = \sqrt{k/\frac{m_{\text{wob}} \cdot m_{\text{rem}}}{m_{\text{wob}} + m_{\text{rem}}}}$$

for a given stiffness k. This simplified assumption predicts resonance at a stiffness value of

$$k_1 = \omega_{\text{stride}}^2 \frac{m_{\text{wob}} \cdot m_{\text{rem}}}{m_{\text{wob}} + m_{\text{rem}}} = 1.33\ Mg/l,$$

which is in good agreement with observed results. Likewise, a second resonance can be predicted when matching the step frequency ω_{step} (which is double the stride frequency) with the wobbling mass oscillation at a spring stiffness of

$$k_2 = \omega_{\text{step}}^2 \frac{m_{\text{wob}} \cdot m_{\text{rem}}}{m_{\text{wob}} + m_{\text{rem}}} = 4 \cdot k_1 = 5.30\ Mg/l.$$

In the actual walker, resonance occurs at a slightly higher stiffness of 5.5 Mg/l, corresponding to the gap between the third and forth solution group in Figure 9-I. For stiffnesses lower than 1.4 Mg/l and higher than 5.5 Mg/l, the wobbling mass oscillated slightly at the step frequency, simply following the excitation from the contact impulses. For resonant oscillations of the wobbling mass relative to a fixed object (as the main body approximates to some degree during the exchange of support), one would predict a stiffness of

$$k_3 = \omega_{\text{stride}}^2 m_{\text{wob}} = 2.21\ Mg/l,$$

which is again in relatively good agreement with the observed second gap at 2.5 Mg/l. As one would expect, the wobbling mass also showed a more pronounced displacement if the spring stiffness was close to these critical values.

We found our prediction of the gap locations were still valid as the fraction of the mass that was allowed to wobble was

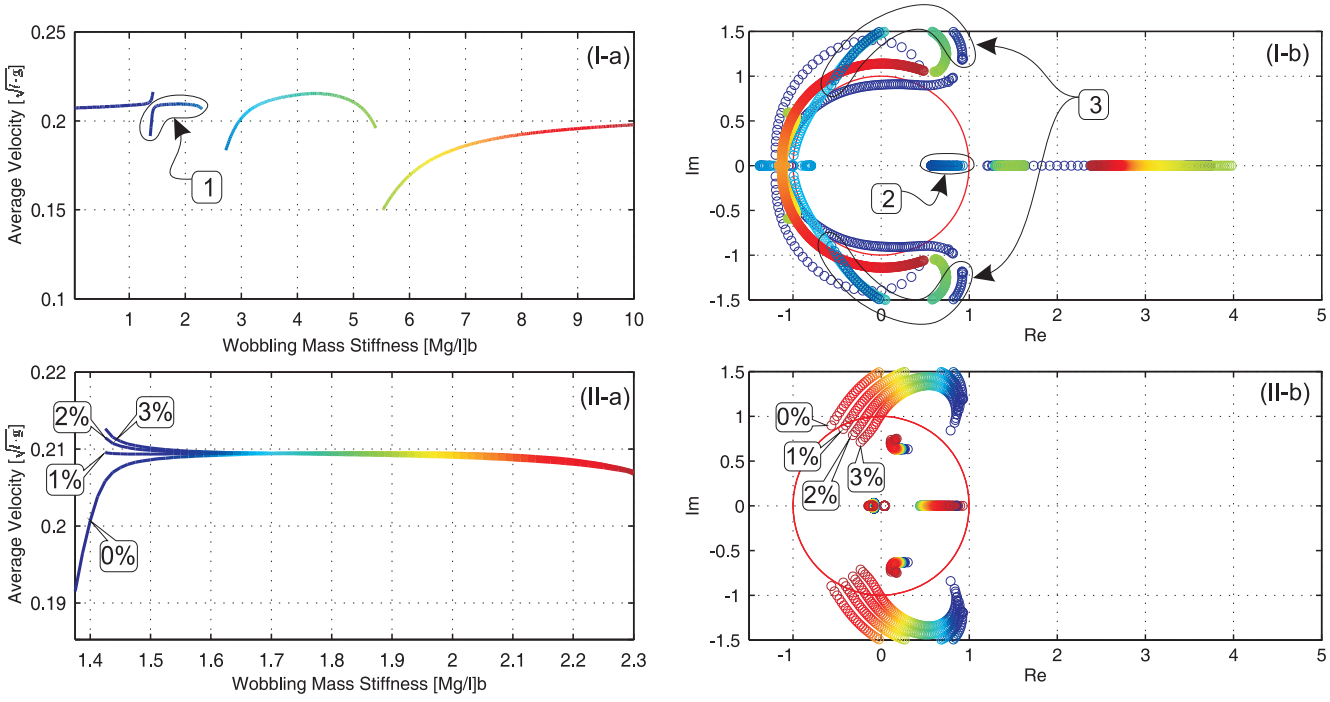

Fig. 9. Shown in (I-b) are the eigenvalues for the phase mode and for the wobbling mass oscillation for increasing stiffness of the wobbling mass connection. The remaining eigenvalues are omitted for clarity. Part (I-a) shows the corresponding walking speed. In contrast to previous plots, distinct solution groups can be identified. If half of the main body's mass is allowed to wobble along the anteroposterior axis with a spring stiffness in the range of 1.4 Mg/l to 2.3 Mg/l (as indicated by label 1), the phase-mode eigenvalue moves inside the unit circle (label 2). However, without damping in the wobbling mass, the additional states create two unstable eigenvalues (label 3). A small amount of damping (values are given as a percentage of the critical damping) can stabilize the eigenvalues of the wobbling mass (II-b) and yield a fully stable, passive, four-beat gait. The achievable walking speed (II-a) was nearly unaffected by the damping. Data markers of the same color in the (a) and (b) plots correspond to the same wobbling mass stiffness.

altered. For wobbling masses of 0.2 M and 0.6 M the same stabilizing behavior was found for stiffness values in the range $[k_1 \ldots k_3]$. Owing to the non-linear dynamical interactions between the wobbling mass, the two pendula motions of the leg pairs, and the contact impulses, it is hard to identify an exact source of the stabilizing effect (or an exact cause for the instability of the phase mode in the original model).

Although the wobbling mass stabilizes the otherwise unstable phase-mode eigenvalue, the two additional eigenvalues (introduced by the expansion of the state space) were unstable with no damping present in the connection to the wobbling mass. Fortunately, a small amount of damping (in the range of just a few per cent of critical damping) was sufficient to move these eigenvalues within the unit circle (Figure 9-II). A slightly damped wobbling mass attached to the main body can thus fully stabilize the quadrupedal four-beat gait.

7. Discussion

The stabilization of the four-beat gait is only a first step in the study of passive dynamics in quadrupedal walking. While the results presented here are significant, the limitations of the model do not allow a complete study of the properties of all possible quadrupedal gaits. Figure 10, for example, displays the large range of gaits that can be found in nature (reproduction of a *gait graph* from Hildebrand (1980)), although even this graph is limited to symmetrical gaits. In a symmetrical gait, all feet are on the ground for the same amount of time and the footfalls within each pair of legs are evenly spaced in time. As a consequence, the left and right side of the body perform the same motion half a stride out of phase and it is sufficient to run the simulation only for a half stride. The symmetrical gaits of Figure 10 are classified by two numbers: the percentage of time each foot stays on the ground during one stride (also called the *duty cycle*) and the phase shift between back and front leg on the same side of the quadruped. Nature utilizes a large range of these gaits (indicated by the shaded

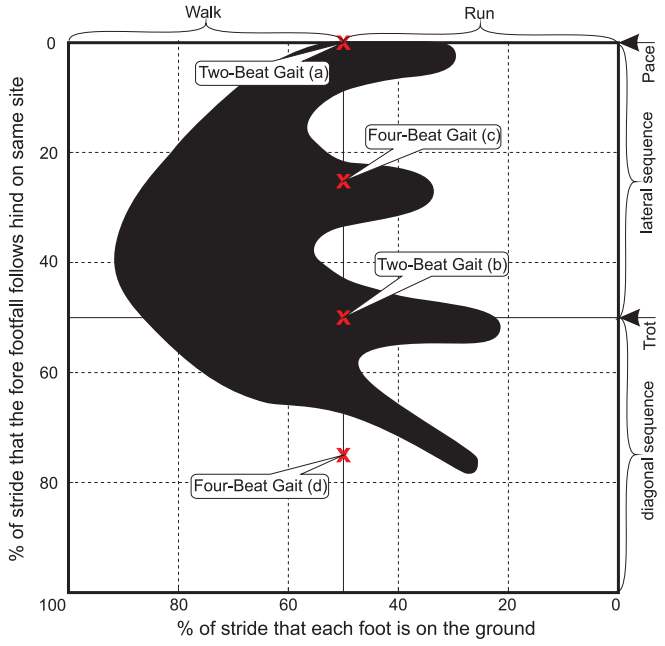

Fig. 10. The two-beat and four-beat gaits (indicated by the four crosses) represent only a few distinct solutions in the continuous range of symmetric gaits found in nature. The percentage of time that each foot is on the ground, and the relative phase of front and back feet are limited in the simplified model. The shaded region was adapted from Hildebrand (1980) and shows the distribution "of more than 1,000 plots for 156 genera of tetrapods". The labels (a)–(d) refer to the footfall sequences depicted in Figure 3 in which the four-beat gaits, "lateral" in (c) and "diagonal" in (d), are characterized by the order of back-foot/front-foot strike sequences on each side of the quadruped.

region) to adapt to various conditions, such as different body geometries, weight, or locomotion speeds. The Hildebrand diagram excludes, for example, asymmetrical bounding or limping gaits, which would require expansion of our half-stride analysis framework to include full-stride period-II motions to be considered.

The simple model presented in this paper is able to reproduce only two gaits: a two-beat gait in which the front and back legs swing in phase, and a four-beat gait in which the leg pairs are acting 90° out of phase. As the legs are perfectly rigid, exactly two legs are in ground contact at all times, which means that the duty cycle is 50% in both cases. The gaits studied here are thus all along the line corresponding to 50% "of stride that each foot is on the ground" in Figure 10. Since the model is planar, no difference between left and right exists. This means that for the two-beat gait a fore footfall is either 0% behind the hind footfall on the same side or 50% behind. For the four-beat gain a fore footfall is either 25% or 75% behind the hind footfall on the same side. These two gaits thus yield a total four points on the graph of Figure 10.

To expand the range of gaits that can be studied, modifications to the model such as those described below are required.

(1) To allow for varying duty cycles, the model must allow for phases in which more or fewer than two legs are in ground contact. The easiest way of doing this within a passive model is by making the legs elastic. The compliance permits the legs to contract, which is necessary for phases of multiple support. The energy stored in the springs is also necessary to perform dynamic push-off that propels the quadruped into the air and allows for phases in which a leg pair is completely off the ground.

(2) To allow for a continuous range of phase shifts, the rigid coupling of the front and back leg dynamics must be eliminated. A possible way of achieving this might be the introduction of elastic elements in the main body segment. Such an elastic body would additionally eliminate the influence of impacts in one leg pair on the other leg pair, thereby eliminating unwanted negative work.

The limitations of a planar model also conceal basic aspects of quadrupedal locomotion. Biological quadrupeds prefer walking gaits (i.e. gaits with a duty cycle less than 50%; see Figure 10) in which the legs fall in a lateral gait sequence rather than in a diagonal gait sequence (see Figure 3 for a definition of *lateral gait sequence*). While equivalent in a planar system, these two gaits create distinctly different support patterns in three dimensions in which the lateral sequence improves static stability by keeping the COM of the quadruped closer to the center of the support polygon. A very good explanation of this issue can be found in Hildebrand (1980). To produce and study such phenomena, the model needs to be expanded (at least partially) to three dimensions. Adding a single degree of freedom and allowing the main body to roll would be a sufficient extension for such a task.

Also not fully clear is the role of parameter asymmetry between front and back (as opposed to side-to-side gait asymmetry), as it is present in almost all living quadrupeds. In our study parameter asymmetry of the model almost inevitably degraded walking performance, which raises the question of whether the asymmetry in nature can be seen as a tradeoff caused by other necessities, or if it becomes beneficial in gaits that cannot be replicated with our simplified model. This is especially interesting, as the possibility of including parameter asymmetry is a key difference between bipedal and quadrupedal locomotion systems.

In terms of modeling elasticity, the expansion of the model to three dimensions allows for an even larger number of possible extensions. Different main body elasticities for lateral stiffness, longitudinal stiffness, and torsional stiffness could enable the system to oscillate in many different modes, which in turn

may correspond to different gaits and could be utilized for different locomotion speeds.

Expanding the range of possible passive motions will be a primary focus of our future research into quadrupedal passive dynamic locomotion. Being able to create the same variety of gaits observed in actual quadrupeds will allow our models to serve as useful references when studying nature or help to exploit passive dynamic principles when building robots. This is especially important in quadrupedal locomotion, where nature utilizes such a rich range of different motions. Stability, performance, and robustness of powered actuation schemes based on insights gained from studies of passive dynamics are also topics for further research and are important to both quadrupedal and bipedal walking.

8. Conclusions

The primary goal of this research has been to develop means of stabilizing the energetically efficient four-beat quadrupedal gait. To that end, a detailed analysis has been presented that examines the influence of various parameters on stability and locomotion speed. Ultimately, stability of the four-beat gait was achieved through the use of a *wobbling mass*, i.e. an additional mass that is elastically attached to the main body of the quadruped. Moreover, the methods, results, and gait analyses presented in this paper provide a point of departure for the exploration of the rich range of quadrupedal locomotion found in nature.

Acknowledgments

This work was supported by the Swiss National Science Foundation (SNF) (project 200021_119965/1) and by the U.S. Office of Naval Research (project N000140810953). The authors gratefully acknowledge Florian Petit for his very valuable preliminary studies of quadrupedal walking while a student at the ETH.

References

Adamczyk, P. G., Collins, S. H. and Kuo, A. D. (2006). The advantages of a rolling foot in human walking. *Journal of Experimental Biology*, **209**(20): 3953–3963.

Bauby, C. E. and Kuo, A. D. (2000). Active control of lateral balance in human walking. *Journal of Biomechanics*, **33**(11): 1433–1440.

Collins, S., Ruina, A., Tedrake, R. and Wisse, M. (2005). Efficient bipedal robots based on passive-dynamic walkers. *Science*, **307**(5712): 1082–1085.

Collins, S.H., Wisse, M. and Ruina, A. (2001). A three-dimensional passive-dynamic walking robot with two legs and knees. *The International Journal of Robotics Research*, **20**(7): 607–615.

Dertien, E. C. (2006). Dynamic walking with Dribbel. *IEEE Robotics and Automation Magazine*, **13**(3): 118–121.

Hildebrand, M. (1980). The adaptive significance of tetrapod gait selection. *International Journal of Computational Biology*, **20**(1): 255–267.

Hof, A. L. (1996). Scaling gait data to body size. *Gait and Posture,* **4**(3): 222–223.

Kuo, A. D. (1999). Stabilization of lateral motion in passive dynamic walking. *The International Journal of Robotics Research*, **18**(9): 917–930.

Liu, W. and Nigg, B. M. (2000). A mechanical model to determine the influence of masses and mass distribution on the impact force during running. *Journal of Biomechanics,* **33**(2): 219–224.

McGeer, T. (1990a). Passive dynamic walking. *The International Journal of Robotics Research* 9(2): 62–82.

McGeer, T. (1990b). Passive walking with knees. *Proceedings of the International Conference on Robotics and Automation*, Vol. 3, pp. 1640–1645.

Osuka, K. and Kirihara, K. (2000). Motion analysis and experiments of passive walking robot QUARTET II. *Proceedings of the International Conference on Robotics and Automation*, Vol. 3, pp. 3052–3056.

Shampine, L. F. and Reichelt, M. W. (1997). *The MATLAB ODE Suite*. Natick, MA: The MathWorks.

Smith, A.C. and Berkemeier, M. D. (1997). Passive dynamic quadrupedal walking. *Proceedings of the International Conference on Robotics and Automation*, Albuquerque, NM, Vol. 1, pp. 34–39.

Vaughan, C. L. and O'Malley, M. J. (2005). Froude and the contribution of naval architecture to our understanding of bipedal locomotion. *Gait and Posture*, **21**(3): 350–362.

Wisse, M., Keliksdal, G., Frankenhyyzen, J. V. and Moyer, B. (2007). Passive-based walking robot. *Robotics and Automation Magazine*, **14**(2): 52–62.

Wood, G. D. and Kennedy, D. C. (2003). *Simulating Mechanical Systems in Simulink with SimMechanics* (91124v00). Natick, MA: The MathWorks.